*sustainability*

MDPI

*Article*

# Spatiotemporal Variations of Extreme Precipitation in Wuling Mountain Area (China) and Their Connection to Potential Driving Factors

**Hong Du [1,*], Jun Xia [2,3], Yi Yan [1], Yumeng Lu [1] and Jinhua Li [1]**

[1] College of Resources and Environmental Science, South-Central Minzu University, Wuhan 430074, China; yanyi@mail.scuec.edu.cn (Y.Y.); 202021241019@mail.scuec.edu.cn (Y.L.); 202021241050@mail.scuec.edu.cn (J.L.)
[2] Chongqing Institute of Green and Intelligent Technology, Chinese Academy of Sciences, Chongqing 400714, China; xiajun@cigit.ac.cn
[3] State Key Laboratory of Water Resources and Hydropower Engineering Science, Wuhan University, Wuhan 430072, China
* Correspondence: 2014021@mail.scuec.edu.cn

**Abstract:** Changes in extreme precipitation have become a significant issue of regional disaster risk assessment and water resources management. Extreme precipitation variability is affected by multiple factors and shows disparities across different regions. Especially in mountain areas, geographic feature and local characteristics put more complexity and uncertainty on the changes of precipitation extremes. In this study, ten extreme precipitation indices of Wuling Mountain Area (WMA) during 1960–2019 have been used to analyzed the spatiotemporal variations of precipitation extremes. The relationships between extreme precipitation and potential driving factors, including geographic factors, global warming, local temperature, and climate indices, were investigated via correlation analysis. The results indicated that extreme precipitation tends to have a shorter duration and stronger intensity in WMA. Decreasing trends in R10mm, R20mm, R25mm, and the consecutive wet days (CWD) series account for 92%, 68%, 52%, and 96% of stations, while most stations in WMA have rising trends in Rx1day (68%), SDII (64%), R95p (72%), and R99p (72%). Significant abrupt changes in extreme precipitation indices mainly occurred in the 1980s–1990s. Geographic factors, local temperature, and climate indices exert different impacts on extreme precipitation. Longitude and elevation instead of latitude significantly affect extreme precipitation indices except for the maximum duration of wet spells. Global warming is likely to increase the intensity and decrease the duration of extreme precipitation, while the influence of local temperature is not exactly the same as that of global warming. The study reveals that summer monsoon indices are the dominant climate factor for variations of precipitation extremes in WMA. The correlation coefficient between extreme precipitation indices (such as Rx1day, R95p, R99p) and the East Asian summer monsoon index is around 0.5 and passed the significant test at the 0.01 level. The weakening of the summer monsoon indices tends to bring extreme precipitation with stronger intensity. The findings provide more understanding of the drivers and reasons of extreme precipitation changes in the mountain area.

**Keywords:** extreme precipitation; spatiotemporal variations; global warming; climate variability; Wuling Mountain Area

check for updates

**Citation:** Du, H.; Xia, J.; Yan, Y.; Lu, Y.; Li, J. Spatiotemporal Variations of Extreme Precipitation in Wuling Mountain Area (China) and Their Connection to Potential Driving Factors. *Sustainability* **2022**, *14*, 8312. https://doi.org/10.3390/su14148312

Academic Editor: Ozgur Kisi

Received: 1 June 2022
Accepted: 3 July 2022
Published: 7 July 2022



## 1. Introduction

Global warming intensifies the hydrologic cycle, and greater atmospheric moisture increases extreme precipitation [1]. The increasing frequency and intensity of precipitation extremes could result in floods [2], soil erosion [3], landslides [4], and other natural disasters, which pose more serious risks and challenges to socio-economic development and human life [5]. Investigating past changes of extreme precipitation and understanding their relationships with the possible driving factors are significant for natural disaster prevention and regional adaptive management.

Many studies have been conducted on the changes of precipitation extremes at the global and regional scales [6,7]. On a global scale, climate warming may bring more evaporation and atmospheric moisture, which leads to more frequent heavy precipitation events. Thus, global extreme precipitation has an increasing trend similar to climate warming [8]. Changes of extreme precipitation in China are consistent with the global trend [9]. However, when it comes to the regional scale, the spatial coherence of trends in extreme precipitation is much weaker than temperature variation [10], and the changes in extreme precipitation are not consistent in different regions and present obvious regional characteristics [11]. An increasing trend in extreme precipitation has been found in the Yangtze River Basin, while extreme precipitation in the Yellow River Basin and northern China shows a decreasing trend [12–14]. Because thermodynamic influences (such as global warming) [15,16] are not the only kind, as dynamic factors (such as climate variability) [17,18] also have an impact on extreme precipitation, and changes in extremes will become larger with the increment of global warming [19]. Dynamic factors can amplify or counteract the thermodynamic influences on extreme precipitation [20]. The role of large-scale atmospheric circulation should be considered to understand regional extreme precipitation variability [21]. In addition, local effects (such as local temperature, geographic factors, land use, urbanization, etc.) [22,23] put more uncertainty on the changes of precipitation extremes. On account of the complicated interaction of thermodynamic, dynamic factors and local effects, the variations of extreme precipitation have spatial heterogeneity in magnitude and direction over different regions [24].

Generally, variations of extreme precipitation have been studied at a large spatial scale, but changes in particular regions have not been conclusive [25]. Regional analysis of different geographical regions is needed to understand the uncertainty of trends in extreme precipitation [26]. Mountain areas are mostly located in the climate transition zone or the terrain transition zone. In addition to global warming and climate factors, geographic features and local effects lead to more complexity and uncertainty to the extreme precipitation changes. Many studies have been carried out on extreme precipitation in mountain areas. Zhang et al. [27] explored the spatial distribution and the temporal trends of the extreme precipitation in the Hengduan Mountains region and found that elevation and the South/East Asian summer monsoon were important influences on precipitation extremes in the mountain region. Shao et al. [5] and Wang et al. [18] studied spatiotemporal variations of extreme precipitation events in the Qinling-Daba mountain region and adopted Pearson correlation analysis method to analyze the correlation between precipitation extremes and geographic, atmospheric factors. The results show extreme precipitation increased in the eastern part of the Qinba mountains while decreased in the western region, and there is a significant correlation between geographic, atmospheric factors and extreme precipitation in the Qinling-Daba mountain region. Zhang et al. [28] analyzed changes in extreme precipitation over the Tienshan Mountains and pointed out that elevation, climate teleconnections, and summer monsoons have an obvious influence on extreme precipitation across the Tienshan Mountains. Thus, not only global warming and climate factors, but also local effects, such as geographic factors and local temperature, should be taken into consideration when studying the changes of extreme precipitation in mountain regions. Meanwhile, reasons or causes of extreme precipitation changes require further exploration in connection with the local characteristics of mountain areas in order to provide a better understanding of the complex extreme precipitation variability in the mountain region.

Located in the eastern extension of Yunnan-Guizhou Plateau, Wuling Mountain Area (WMA) is an important water conservation area and ecological barrier of the Yangtze River Basin. Compared with other parts of the Yangtze River Basin, WMA is the terrain transition zone with frequent natural disasters and high ecological vulnerability. It is a typical mountain region sensitive to extreme climate events. Natural disasters frequently occur in this area and lead to huge disaster losses. Precipitation extremes and the resulting flood disaster are one of the most frequent, longest lasting, and most extensive damage disasters in WMA, which seriously restricts the realization of the strategic goal of poverty alleviation and Rural Revitalization in Ethnic Minority Areas. So far, the extreme precipitation events and flood disasters are intensified under global climate warming. Especially since the 1990s, extreme precipitation and flood events in WMA have happened more frequently, which bring about severe losses. In June 2017, WMA suffered continuous rainstorms. In Huaihua City alone, there were 182 towns with 570,800 people suffering from the disaster, leading to 1.31 billion RMB of direct economic loss [29]. Although there have been many investigations on changes of extreme precipitation and influencing factors over the Yangtze River Basin [30,31], there have been very few studies on the changes in extreme precipitation in the Wuling Mountain Area (WMA). Meanwhile, the association between the variations in precipitation extremes and influencing factors, such as global warming, local effects, and ENSO, have been explored in the Yangtze River Basin [32,33]. However, the influences of the potential driving factors on the extreme precipitation over the basin remain unknown. As with the spatial heterogeneity and inconsistency, as well as local effects, the previous studies on the Yangtze River Basin are not adequate to provide detailed information about precipitation extremes in WMA. Thus, it is still desirable to explore the extreme precipitation changes and the possible connections between the precipitation extremes and potential influencing factors in WMA.

This study aims to explore the spatiotemporal patterns of precipitation extremes variations in WMA and attempts to examine the possible associations between precipitation extremes changes and likely driving factors over the region using the high-quality daily precipitation data and potential influencing factors' data during 1960–2019. The findings of our study may enhance our understanding of the complicated extreme precipitation changes and their connections with potential driving factors and reveal the main cause of extreme precipitation variability, which is critical and helpful for natural disaster prevention and mitigation and adaptive water resources management in mountain area.

## 2. Study Area and Data

### *2.1. Study Area*

WMA is located between 25°52′–31°24′ N and 107°4′–112°2′ E. It covers an area of 171,800 km$^2$ and includes 71 counties (cities, districts) in the border areas of Hubei, Chongqing, Hunan, and Guizhou provinces. It belongs to the mountainous area where the subtropical zone is transitional to the warm temperate zone in China. The area's terrain is high in the northwest and low in the southeast, with an average altitude of 1000 m. The annual average temperature in WMA is 12–17 °C, and the annual precipitation is 1100–1600 mm. There is abundant precipitation but uneven distribution in the year. Precipitation from May to August takes up more than 50% of the total annual precipitation, which is prone to flood disasters. Especially under the influence of climate warming, the occurrence of precipitation extremes and floods in WMA shows an increasing trend. The location of WMA and the distribution of meteorological stations in WMA are shown in Figure 1.

### *2.2. Data*

#### 2.2.1. Precipitation and Geographic Factors

The daily precipitation data of the 25 selected meteorological stations during 1960–2019 in WMA were obtained from the China Meteorological Data Service Center (http://data.cma.cn/, accessed on 1 July 2020). The original data files are subjected to rigorous quality control and inspection. Additional information for the selected meteorological stations is supplied in Table 1, and their locations are displayed in Figure 1.

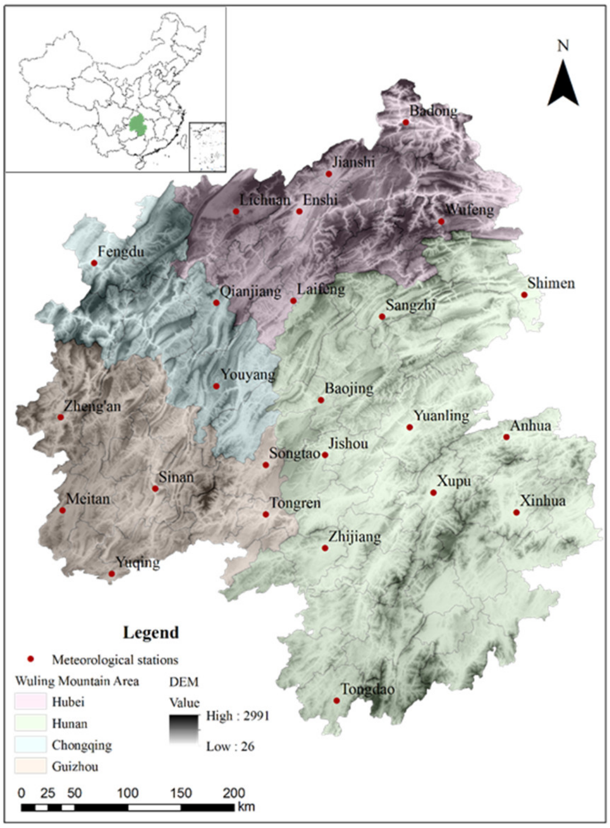


**Figure 1.** The location of WMA and the distribution of meteorological stations in WMA.

**Table 1.** Details of the selected meteorological stations in WMA.

| ID | Station Name | Province | Latitude (°N) | Longitude (°E) | Elevation (m) |
|---|---|---|---|---|---|
| 1 | Fengdu | Chongqing | 29.85 | 107.73 | 290.5 |
| 2 | Qianjiang | Chongqing | 29.52 | 108.77 | 786.9 |
| 3 | Youyang | Chongqing | 28.82 | 108.77 | 826.5 |
| 4 | Meitan | Guizhou | 27.77 | 107.47 | 792.2 |
| 5 | Tongren | Guizhou | 27.73 | 109.18 | 353.2 |
| 6 | Sinan | Guizhou | 27.95 | 108.25 | 416.8 |
| 7 | Songtao | Guizhou | 28.15 | 109.18 | 406.1 |
| 8 | Yuqing | Guizhou | 27.23 | 107.88 | 622.1 |
| 9 | Zheng'an | Guizhou | 28.55 | 107.45 | 679.7 |
| 10 | Badong | Hubei | 31.03 | 110.37 | 334.0 |
| 11 | Enshi | Hubei | 30.28 | 109.47 | 457.1 |
| 12 | Jianshi | Hubei | 30.60 | 109.72 | 609.2 |
| 13 | Laifeng | Hubei | 29.53 | 109.42 | 502.8 |
| 14 | Lichuan | Hubei | 30.28 | 108.93 | 1074.1 |
| 15 | Wufeng | Hubei | 30.20 | 110.67 | 619.9 |
| 16 | Anhua | Hunan | 28.38 | 111.22 | 128.3 |
| 17 | Baojing | Hunan | 28.70 | 109.65 | 325.3 |
| 18 | Jishou | Hunan | 28.23 | 109.68 | 254.6 |
| 19 | Sangzhi | Hunan | 29.40 | 110.17 | 322.2 |
| 20 | Shimen | Hunan | 29.58 | 111.37 | 116.9 |
| 21 | Tongdao | Hunan | 26.17 | 109.78 | 397.5 |
| 22 | Xinhua | Hunan | 27.75 | 111.30 | 211.9 |
| 23 | Xupu | Hunan | 27.92 | 110.60 | 204.0 |
| 24 | Yuanling | Hunan | 28.47 | 110.40 | 151.6 |
| 25 | Zhijiang | Hunan | 27.45 | 109.68 | 272.2 |

Geographic factors are one of the potential elements affecting precipitation. There is a definite association between precipitation and elevation [34]. Generally speaking, precipitation increases gradually with elevation; however, it may decline over a certain height. Meanwhile, latitude determines the pressure zone and the wind zone, and it may have an indirect effect on precipitation. In this study, the latitude, longitude, and elevation of the meteorological stations (shown in Table 1) are chosen as geographic factors to analyze its relationship with extreme precipitation in WMA.

### 2.2.2. Extreme Precipitation Indices

Different extreme precipitation indices may have dissimilar variations and responses to a specific driving factor, therefore frequency-based indices, duration-based indices, and intensity-based indices are used to represent extreme precipitation. Based on the daily precipitation data, ten extreme precipitation indices are selected to describe extreme precipitation events according to the recommendation of the Expert Team on Climate Change Detection and Indices (ETCCDI). Under the classification method in [23] and [35], these ten precipitation extremes indices can be categorized into frequency-based, duration-based, and intensity-based indices (Table 2).

**Table 2.** Descriptions of extreme precipitation indices used in the study.

| Indices Categories | Indices Abbreviation | Name | Definition | Unit |
|---|---|---|---|---|
| Frequency-based indices | R10mm | Days of heavy precipitation | Annual total days when precipitation $\geq$ 10 mm | days |
| | R20mm | Days of very heavy precipitation | Annual total days when precipitation $\geq$ 20 mm | days |
| | R25mm | Days of extremely heavy precipitation | Annual total days when precipitation $\geq$ 25 mm | days |
| Duration-based indices | CWD | Consecutive wet days | Maximum length of consecutive wet days (daily precipitation $\geq$ 1 mm) | days |
| Intensity-based indices | Rx1day | Maximum 1-day precipitation | Annual maximum 1-day precipitation | mm |
| | Rx5day | Maximum 5-day precipitation | Annual maximum consecutive 5-day precipitation | mm |
| | SDII | Simple daily intensity index | Annual total wet-day precipitation divided by the number of wet days | mm/day |
| | R95p | Precipitation in very wet days | Annual total precipitation when daily precipitation > 95th percentile | mm |
| | R99p | Precipitation in extremely wet days | Annual total precipitation when daily precipitation > 99th percentile | mm |
| | PRCPTOT | Annual total wet day precipitation | Annual total precipitation on wet days | mm |

### 2.2.3. Global Warming and Local Temperature

The near-surface temperature at global and local scales are used as indicators for global warming and local warming, respectively [22,23]. They are obtained from the National Aeronautics and Space Administration (http://data.giss.nasa.gov/gistemp/, accessed on 1 July 2020) and China Meteorological Data Service Center (http://data.cma.cn/, accessed on 1 July 2020).

### 2.2.4. Climate Indices

Pacific Decadal Oscillation (PDO), Southern Oscillation Index (SOI), Arctic Oscillation (AO), North Atlantic Oscillation (NAO), Northern Oscillation Index (NOI), and the Multivariate ENSO Index (MEI) are potential climate factors influencing the climate in

China [5,36,37]; therefore, these factors are selected as the climate indices in this study. They are extracted from the United States National Oceanic and Atmospheric Administration (http://www.esrl.noaa.gov/psd/data/climateindices/list/, accessed on 1 July 2020). Moreover, the monsoon is another close link with precipitation extremes in China. The South China Sea summer monsoon index (SCSSMI) and East Asian summer monsoon index (EASMI) were used in the study, which were downloaded from http://lijianping.cn/dct/page/1, accessed on 1 July 2020.

## 3. Methodology

### *3.1. Mann-Kendall Trend Test*

Mann–Kendall test (M-K test) is less sensitive to outliers and does not require data to follow a specific distribution, therefore it has been widely used to detect trends in hydrometeorological time series [38,39]. In order to eliminate the influence of serial correlation, the pre-whitening method proposed by Yue et al. [40] is used in the M-K test in the study. The results of the M-K trend test are judged by statistical parameter Z. $Z > 0$ indicates that the time series has an increasing trend, while $Z < 0$ suggests that the time series has a decreasing trend. The significant level used in the study is 0.05. Thus, if $|Z| \geq 1.96$, the trend is significant at the 95% confidence level [41]. The detailed information of the M-K test is available in [42,43].

### *3.2. Pettit Abrupt Test*

Pettitt test is a kind of nonparametric change-point test employed to detect a single change-point in time series without presupposing the location of the change point [44]. It detects the rank-sum sequence of the original data, reducing the influence of outliers. Meanwhile, the statistical significance level of the abrupt changes can be quantified in the Pettitt test [45]. When the significance level is set at $\alpha = 0.05$, the test statistic $p$-value $< 0.05$ indicates that no apparent abrupt occurs in the time series. The $p$-value calculation procedures are available in detail in [46].

### *3.3. Pearson's Correlation Analysis*

Pearson's correlation analysis method is a simple and effective way to measure linear independence between two variables, which reflects not only the magnitude of the correlation, but also the significance of the correlation. It is widely used to analyze the connections between extreme precipitation and related influencing factors [18,23]. The Pearson correlation coefficient [14] has been commonly used to indicate the linear relationship between two variables. The correlation coefficient value is between $-1$ and 1. When the correlation coefficient value is greater than zero, there is a positive correlation between two variables, whereas there is a negative correlation when the coefficient is less than zero. If the coefficient is equal to zero, it indicates no linear relationship between the two variables. The closer the coefficient is to 0, the lower the linear correlation magnitude, while the closer the coefficient is to $-1$ or 1, the higher the linear correlation magnitude. Pearson's correlation analysis is used to determine the impact of the potential influencing factors on precipitation extremes in WMA.

## 4. Results

### *4.1. Spatial and Temporal Variations of Extreme Precipitation*

#### 4.1.1. Trends in Extreme Precipitation Indices

Spatial variation features of annual average extreme precipitation indices show many similarities except CWD (Figures 2 and S1).

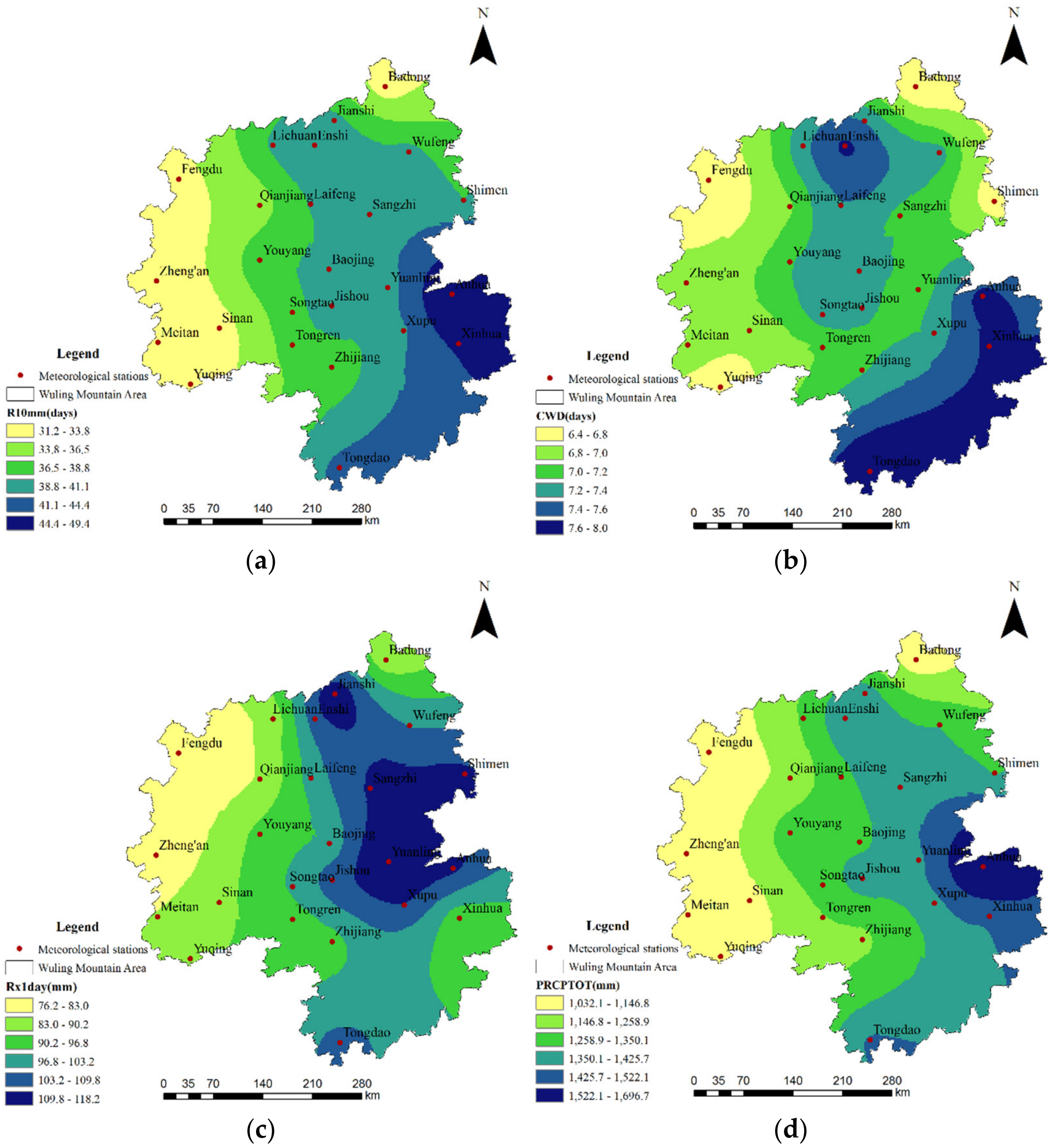


**Figure 2.** Spatial variations of annual average extreme precipitation indices: (**a**) R10mm, (**b**) CWD, (**c**) Rx1day, and (**d**) PRCPTOT in WMA.

The high values of CWD emerge in the southeast and north part of WMA, while the low values of CWD occur in the northeast and west part of WMA. CWD gradually decreases from southeast to northwest, and from north to other directions. For other extreme precipitation indices, there is a similar decreasing trend from east to west, or from southeast to northwest of WMA. Meanwhile, in the northeast of WMA, a downward trend emerges from the middle part of WMA to the northeast region. The spatial changes of average annual PRCPTOT are generally consistent with the results from [47]. PRCPTOT is significantly correlated with all the selected precipitation extremes indices except CWD, therefore almost all indices display similarities in spatial variations except CWD. Furthermore, it indicates that the annual total precipitation has good correlations with extreme precipitation. By contrast, CWD is weakly correlated with precipitation extremes. Besides, the trend magnitudes of all extreme precipitation indices except CWD in WMA have significant correlations with longitude rather than latitude, which reveals the influence of geographic factors on spatial changes of extreme precipitation indices in WMA.

The percentage of stations with different trends and the spatial distribution of trends in the selected ten extreme precipitation indices in WMA are shown in Figures 3, 4 and S2. Frequency-based indices, such as R10mm, R20mm, and R25mm, are able to reflect the frequency of extreme precipitation. Moreover, 92%, 68%, and 52% of stations in the WMA show decreasing trends of R10mm, R20mm, and R25mm series, respectively. It indicates that the frequencies of extreme precipitation reduce at most sites in the WMA. Ninety-six percent of stations display declining trends of consecutive wet days (CWD), and 50% (12 stations) passed the significance test. It suggests the annual maximum length of wet days tends to shorten. However, most stations in WMA have rising trends in Rx1day (68%), SDII (64%), R95p (72%), and R99p (72%). Although slightly more stations (13 stations) show a downward trend for Rx5day, there are fewer stations with a significant negative trend (4 stations) than those with an apparent positive trend (12 stations). The results reveal that the intensities of average precipitation (SDII) and extreme precipitation (Rx1day, R95p, R99p) in WMA have increased obviously from 1960 to 2019. However, the opposite occurs in the annual total precipitation in wet days (PRCPTOT). Downward trends are found in PRCPTOT at 14 stations, which are mainly distributed in the west and north part of WMA. Further, the frequency of extreme precipitation (represented by R20mm and R25mm, see in Figure S2) tend to increase in the middle and east of WMA, where there are areas with relatively low topography and high extreme precipitation intensity. Additionally, the precipitation extremes with a shorter duration but higher intensity are more likely to happen in WMA, which may lead to floods, landslide, and debris flow, posing a greater challenge to disaster prevention and mitigation in the region.

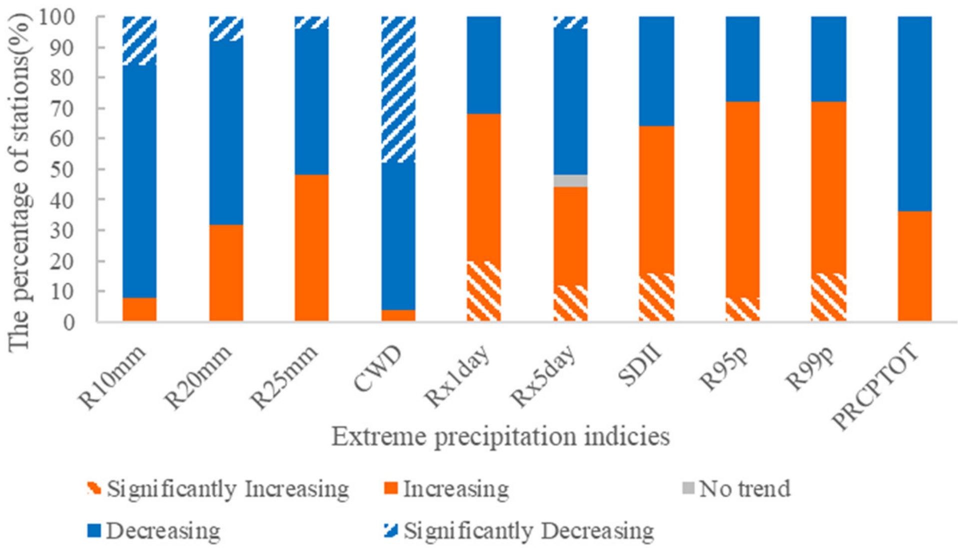


**Figure 3.** The percentage of stations with different trends in extreme precipitation indices.

In terms of the regional average extreme precipitation indices in WMA (Figure 5), R10mm, R20mm, and R25mm show increasing trends at a regional average of 0.6 days/decade, 0.2 days/decade, 0.1 days/decade, respectively; however, the increasing trends did not pass the significance test at the 0.05 significance level. With an increase in the precipitation threshold, the ten-year change rate of the frequency-based indices gradually decreases, so too does the significance of the decreasing trend. Regional average CWD has an obviously decreasing trend with 0.03days/decade. Rx1day, Rx5day, SDII, R95p, and R99p show a rising trend, and the upward trend of R99p is apparent. PRCPTOT displays a downward trend at a regional average of 4.8 mm/decade. Regional trend analysis results of extreme precipitation in WMA are basically in line with at-site analysis results.

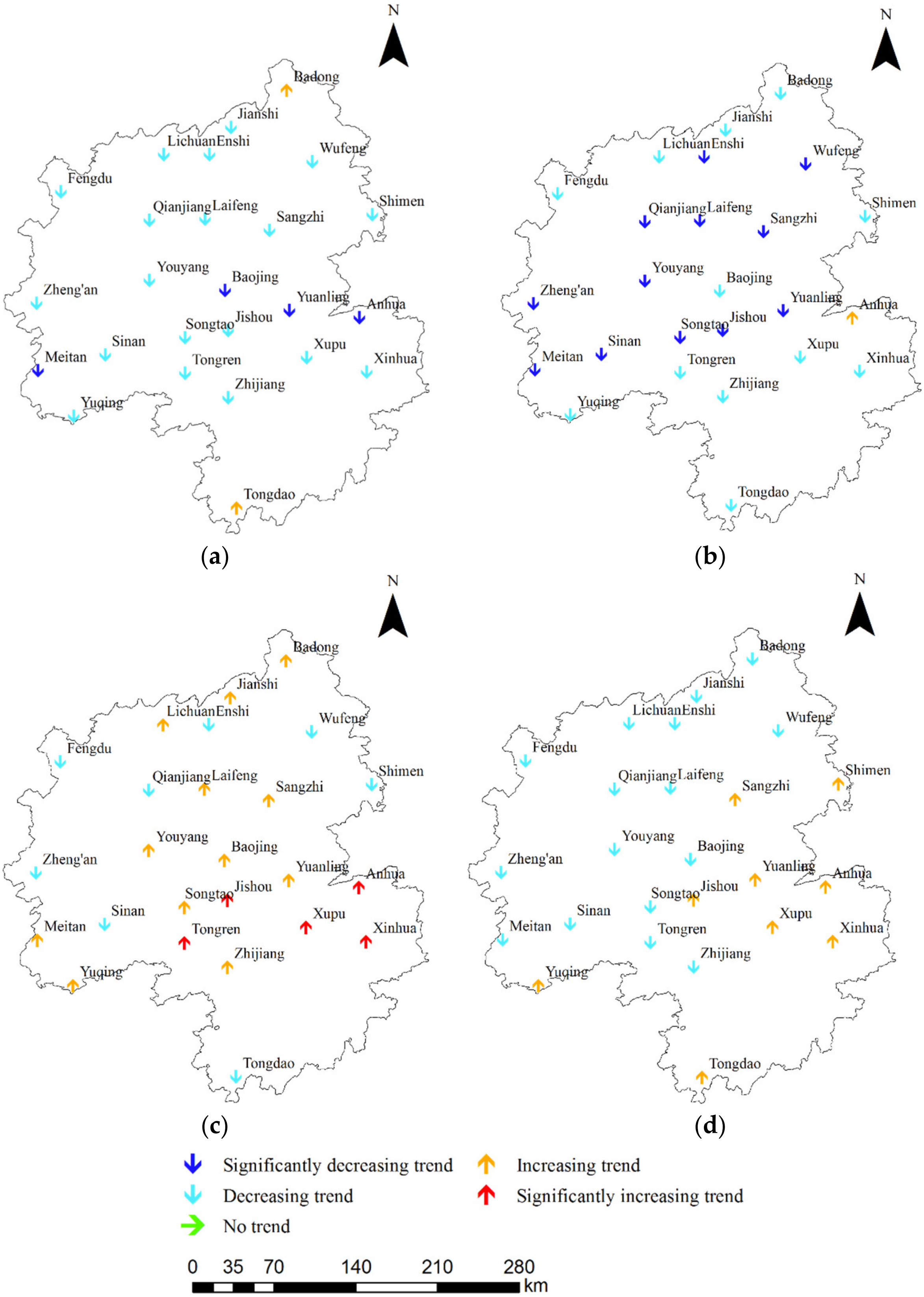


**Figure 4.** Spatial distribution of trends in extreme precipitation indices: (**a**) R10mm, (**b**) CWD, (**c**) Rx1day, and (**d**) PRCPTOT in WMA.

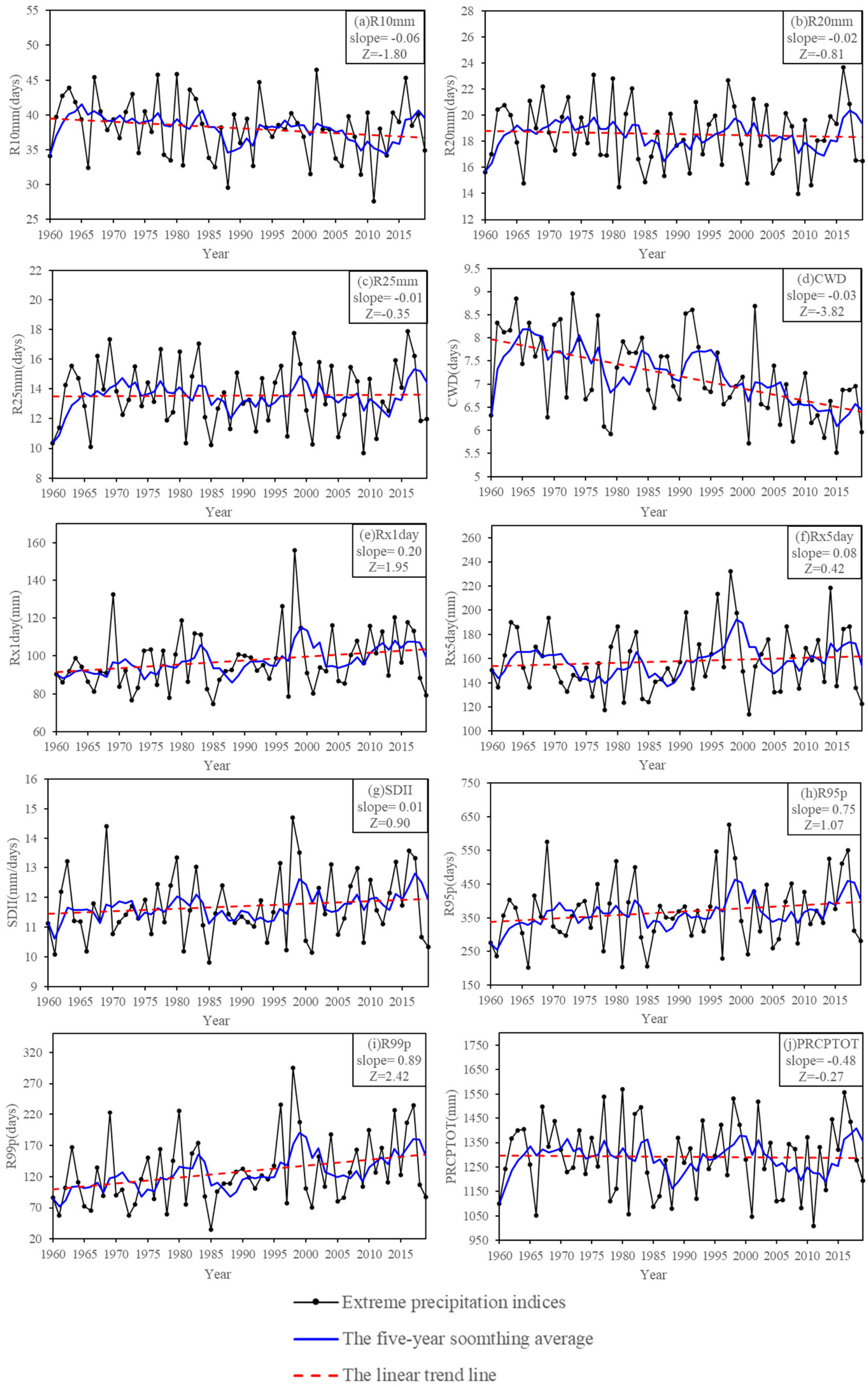


**Figure 5.** Trends of regional average extreme precipitation indices in WMA (Slope is the slope of the linear trend line; Z is a statistical parameter in M-K trend test).

4.1.2. Abrupt Changes in Extreme Precipitation Indices

From Figure S3, for R20mm, R25mm, SDII, and PCRPTOT, there is no significant abrupt changes detected in WMA. For R10mm, an obvious abrupt change was found at Songtao, Meitan in 1985. There are abrupt changes found in 1988, 1987, and 1987 for R95p, Rx1, and Rx5 at Anhua, which represent that the significant abrupt of precipitation extremes indices at Anhua emerged around 1987. For R99p and Rx1day, abrupt changes are detected in 1994 and 1992 at Zhijiang and Xupu, respectively. Rx5day at Xupu is found to be abrupt in 1988. In terms of CWD, significant abrupt changes are seen at nine stations, that is, Qiangjiang and Sinan in 1978, Zheng'an in 1983, Sangzhi in 1985, Songtao in 1993, Shimen and Jishou in 1994, Enshi and Youyang in 1997.

From Figure 6, during the 1960s, 2000s, and 2010s, no obvious abrupt changes were found in all selected extreme precipitation indices. In the 1970s, abrupt changes in CWD at Qianjiang and Sinan were detected. There are two stations for R10mm (Songtao, Meitan), CWD (Zheng'an, Sangzhi), Rx5day (Anhua, Xinhua), and one station (Anhua) for Rx1day, R95p was found to have significant abrupt changes in the 1980s. Moreover, in the 1990s, abrupt changes emerged at Enshi, Shimen, Youyang, Songtao, and Jishou for CWD, at Xupu and Xinhua for Rx1day and R99p, respectively. The stations detected obvious abrupt changes distributed in the high-value region of extreme precipitation for Rx1day, Rx5day, R99p. In contrast, for CWD, the stations with significant abrupt mainly emerge in the middle part of WMA.

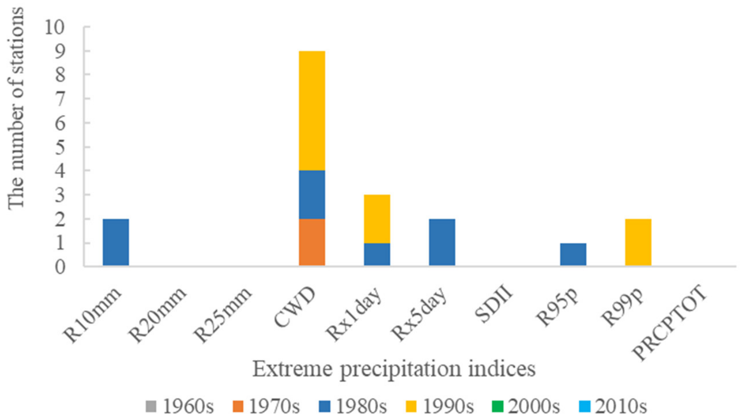


**Figure 6.** The number of stations with abrupt changes in extreme precipitation indices in WMA.

For the regional average extreme precipitation indices, only one significant abrupt change ($p$-value < 0.05) was detected in 1997 of the CWD series (Figure 7). There are no obvious abrupt changes in the other regional averages of extreme precipitation indices series under the significance levels at $\alpha = 0.05$.

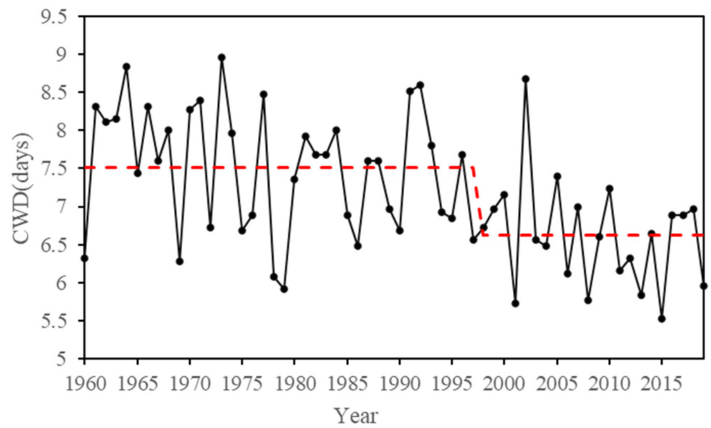


**Figure 7.** Abrupt changes detected of the regional average of annual CWD series.

### *4.2. Correlation with Potential Factors*

#### 4.2.1. Correlation between Extreme Precipitation Indices

From the analysis of previous trends of extreme precipitation in WMA, many extreme precipitation indices show similarities in variations. Thus, the correlation between precipitation extremes indices in WMA during 1960–2019 is analyzed first. As shown in Table 3, all the extreme precipitation indices except CWD show significantly positive correlations with annual total precipitation PRCPTOT (correlation coefficient > 0.60, $p < 0.01$), and CWD showed a weak correlation with PRCPTOT (correlation coefficient = 0.28, $p < 0.05$). Furthermore, CWD is weakly correlated with other precipitation extremes except for R10mm. The results are a good illustration of spatial variations of average annual extreme precipitation indices shown in Figure 2 and Figure S1, which is that almost all indices display similarities in spatial variations except CWD.

**Table 3.** Correlation between extreme precipitation indices.

| | **R10mm** | **R20mm** | **R25mm** | **CWD** | **Rx1day** | **Rx5day** | **SDII** | **R95p** | **R99p** | **PRCPTOT** |
|---|---|---|---|---|---|---|---|---|---|---|
| R10mm | 1.00 | 0.84 ** | 0.77 ** | 0.42 ** | 0.30 * | 0.46 ** | 0.44 ** | 0.50 ** | 0.39 ** | 0.91 ** |
| R20mm | | 1.00 | 0.97 ** | 0.18 | 0.61 ** | 0.66 ** | 0.78 ** | 0.81 ** | 0.69 | 0.95 ** |
| R25mm | | | 1.00 | 0.14 | 0.70 ** | 0.73 ** | 0.84 ** | 0.89 ** | 0.77 ** | 0.94 ** |
| CWD | | | | 1.00 | −0.11 | 0.09 | −0.09 | −0.02 | −0.11 | 0.28 * |
| Rx1day | | | | | 1.00 | 0.83 ** | 0.83 ** | 0.89 ** | 0.95 ** | 0.63 ** |
| Rx5day | | | | | | 1.00 | 0.78 ** | 0.85 ** | 0.84 ** | 0.70 ** |
| SDII | | | | | | | 1.00 | 0.93 ** | 0.88 ** | 0.69 ** |
| R95p | | | | | | | | 1.00 | 0.94 ** | 0.80 ** |
| R99p | | | | | | | | | 1.00 | 0.71 ** |
| PRCPTOT | | | | | | | | | | 1.00 |

Note: * and ** denote significant correlation at the 0.05 and 0.01 levels, respectively.

Meanwhile, the extremely strong correlated indices with PRCPTOT are R10mm, R20m, and R25mm, with the correlation coefficients of 0.91, 0.95, and 0.94. It indicates that the decrease in R20mm contributed to the downward trend of PRCPTOT in WMA over 1960–2019, and that the frequency-based indices (R10mm, R20mm, R25mm) are strong and significantly correlated with each other. The same is true for intensity-based indices. There is not a strong correlation between frequency-based and intensity-based indices. Still, all the correlations are evident at a 0.01 level except that correlation between R10mm and Rx1day is obvious at a 0.05 level. Moreover, R10mm is not as strongly correlated with intensity-based indices as R20m and R25mm.

#### 4.2.2. Correlation with Geographic Factors

The potential influence of geographic factors on the extreme precipitation indices in WMA is explored via Pearson's correlation analysis. From the results shown in Table 4, all extreme precipitation indices have positive correlations with longitude in WMA, and these correlations are significant at 0.01 significant level with the exception of CWD. There is a powerful positive correlation between SDII and longitude, and the correlation coefficient between SDII and longitude is 0.90—the highest among correlation coefficients between extreme precipitation indices and longitude. These results indicate that longitude is one of the significant influence factors for extreme precipitation indices in WMA.

Obvious correlations are also observed between most extreme precipitation indices and elevation. Extreme precipitation indices show negative correlations with elevation except for CWD, making it clear that extreme precipitation variations decrease with increasing elevation. Moreover, the correlation between R20mm, R25mm, Rx1day, Rx5day, R95p, and R99p with altitude passes the significant test at the significance level of 0.05. The correlation between SDII and altitude is evident at the significance level of 0.01. Furthermore, the correlation coefficient between SDII and altitude is −0.63, the absolute value of which is higher than the correlation coefficients between altitude and other extreme precipitation indices. These results indicate that altitude is significantly correlated with the extreme precipitations during 1960–2019 in WMA.

**Table 4.** Correlation between extreme precipitation indices and geographic factors.

| Extreme Precipitation Indices | Longitude | Latitude | Altitude |
|---|---|---|---|
| R10mm | 0.76 ** | −0.07 | −0.39 |
| R20mm | 0.80 ** | 0.00 | −0.42 * |
| R25mm | 0.80 ** | 0.00 | −0.45 * |
| CWD | 0.30 | −0.20 | 0.06 |
| Rx1day | 0.70 ** | 0.02 | −0.49 * |
| Rx5day | 0.76 ** | −0.03 | −0.46 * |
| SDII | 0.90 ** | 0.16 | −0.63 ** |
| R95p | 0.69 ** | −0.19 | −0.45 * |
| R99p | 0.53 ** | −0.33 | −0.42 * |
| PRCPTOT | 0.76 ** | −0.05 | −0.39 |

Note: * and ** denote significant correlation at the 0.05 and 0.01 levels, respectively.

However, the correlations between latitude and extreme precipitation indices are fairly weak. R10mm, CWD, Rx5day, R95p, R99p, and PRCPTOT show negative correlations with latitude, while Rx1day and SDII show positive correlations with latitude in WMA. Moreover, these correlations are not apparent at the 0.05 level. There are no correlations detected between R20mm and R25mm with latitude.

Thus, all extreme precipitation indices except CWD in WMA are well correlated with longitude and elevation rather than latitude, which is in accord with the results shown in Figure 2 and Figure S1. Meanwhile, the study confirms that mountainous and highland areas are very sensitive and vulnerable to extreme weather and extreme hydrological events [48,49]. Altitude has an obvious negative correlation with almost all extreme precipitation indices in WMA. The higher the altitude, the smaller the extreme precipitation.

#### 4.2.3. Correlation with Global Warming and Local Temperature

The correlation between regional average extreme precipitation indicators and global temperature is shown in Table 5. Except for R10mm and CWD, there is a positive correlation between other extreme precipitation indices and global temperature. The correlation between R99p and global temperature is obvious at a significant level of 0.01, and the correlation between Rx1day and global temperature passes the test with a significant level at 0.05. However, CWD is negatively correlated with global temperature, which is significant at the 0.01 level.

**Table 5.** Correlation between regional average extreme precipitation indicators and global temperature.

| Extreme Precipitation Indices | Global Temperature |
|---|---|
| R10mm | −0.10 |
| R20mm | 0.02 |
| R25mm | 0.08 |
| CWD | −0.48 ** |
| Rx1day | 0.26 * |
| Rx5day | 0.13 |
| SDII | 0.20 |
| R95p | 0.21 |
| R99p | 0.34 ** |
| PRCPTOT | 0.05 |

Note: * and ** denote significant correlation at the 0.05 and 0.01 levels, respectively.

Figures 8 and S4 show the spatial pattern of the correlation between extreme precipitation indices and global temperature. It is basically in line with the correlation results between regional average annual extreme precipitation indices and global temperature reported in Table 5. A prevailing negative correlation pattern between R10mm, CWD, and the global temperature can be seen in WMA. However, the negative correlation between R10mm and the global temperature is non-significant at the 0.05 level, and the absolute value of correlation coefficients are less than 0.3, which indicates weak connection. Moreover, the correlation between CWD and the global temperature is marked negative at the 0.05 level over the entire region. There is strong and significant negative correlation at Youyang station, with the correlation coefficient ranging from −0.5 to −0.4. However, a dominant positive correlation can be found between Rx1day, Rx5day, SDII, R95p, R99p, and the global temperature, in which some stations in the southeast of WMA pass the significant test at the 0.05 level. Besides, the positive and negative correlations between R20mm, R25mm, PRCPTOT, and the global temperature are evenly balanced. There are 13 stations (52%), 14 stations (56%), and 12 stations (48%) with a positive correlation between R20mm, R25mm, PRCPTOT, and the global temperature, respectively. Generally, stations in the east show a positive relationship, while that in the west display a negative pattern over WMA for correlations between R20mm, R25mm, PRCPTOT, and the global temperature. The results indicate that climate warming reinforces the intensity of extreme precipitation in WMA. However, climate warming demonstrates a significant tendency to reduce the maximum consecutive wet days over WMA. Additionally, climate warming inclines to raise the frequency of precipitation extremes in the east of WMA yet diminish the frequency of precipitation extremes in the west of WMA.

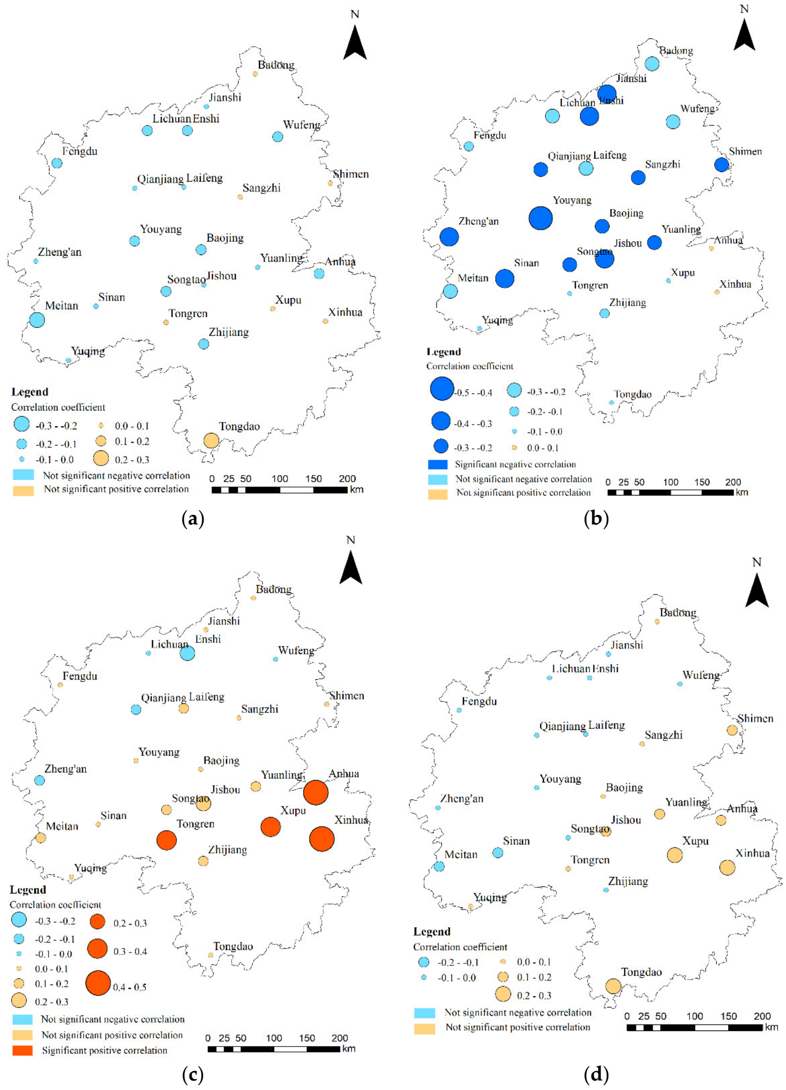


**Figure 8.** Spatial pattern of correlation between extreme precipitation indices (**a**) R10mm, (**b**) CWD, (**c**) Rx1day, (**d**) PRCPTOT, and global temperature in WMA.

The spatial distribution of correlation between the extreme precipitation indices and local temperature is displayed in Figures 9 and S5. There is a negative control correlation between local temperature and R10mm, R20mm, R25mm, CWD, R95p, and PRCPTOT, while most stations show a positive correlation with local temperature in terms of Rx1day, R99P, and SDII. There are 14 stations (56%) with a negative correlation between local temperature and Rx5day. Thus, for R10mm, CWD, Rx1day, R99p, SDII, and PRCPTOT, the spatial pattern of correlation between the extreme precipitation indices and local temperature is generally in agreement with that of the extreme precipitation indices–global temperature correlation. Moreover, for the other four extreme precipitation indicators, the spatial feature of the extreme precipitation indices–local temperature correlation is opposed to that of the extreme precipitation indices–global temperature correlation. These results show that local warming tends to reduce not only the frequency of extreme precipitation and the maximum length of wet days, but also annual total precipitation and very wet days precipitation. However, local warming tends to increase maximum one-day precipitation, extremely very wet days precipitation, and the intensity of the precipitation.

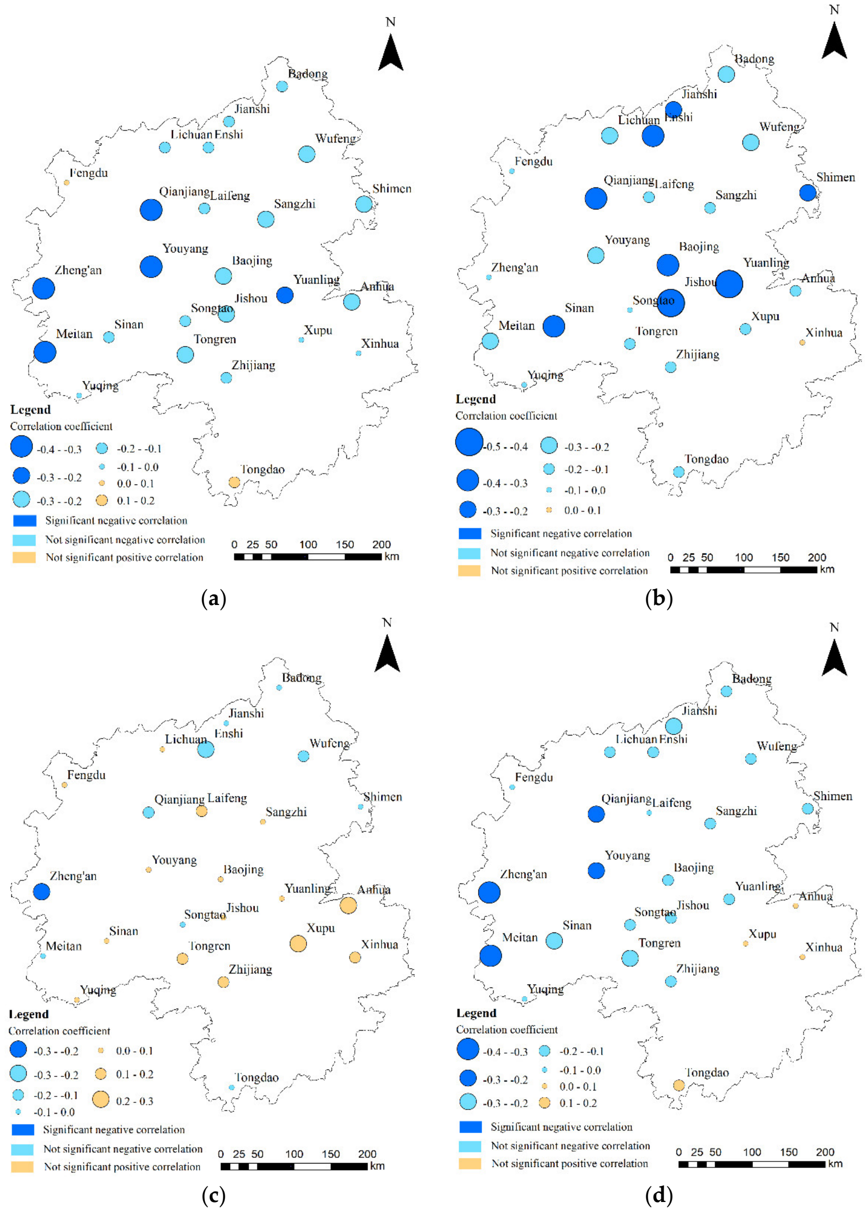


**Figure 9.** Spatial pattern of correlation between extreme precipitation indices (**a**) R10mm, (**b**) CWD, (**c**) Rx1day, (**d**) PRCPTOT, and local temperature in WMA.

### 4.2.4. Correlation with Climate Indices

From Figure 10, except R10mm and CWD, there are positive correlations between extreme precipitation indicators and AO. Meanwhile, positive correlations can also be found between PDO and extreme precipitation indicators, except for CWD. However, the negative correlations emerge between NAO and extreme precipitation, except for R95p. The NAO-extreme precipitation correlation and MEI-extreme precipitation correlation move in the opposite direction, except for CWD and Rx5day. Yet, the PDO-extreme precipitation correlation and MEI-extreme precipitation correlation are in the same direction, except for Rx5day and R95p. The correlation coefficients of extreme precipitation and AO, SOI, NAO, PDO, NOI, and MEI are small and do not pass the test at the significant level of 0.05 and 0.01. It implies that the influence of these climate factors on precipitation extremes is relatively weak and limited in WMA over 1960–2019. Except CWD, EASMI has a negative correlation with other extreme precipitation indices, in which marked negative correlations are found with R25mm, Rx1day, Rx5day, SDII, R95p, R99p (significant at 0.01 level), R20mm, and PRCPTOT (significant at 0.05 level). Another summer monsoon index SCSSMI exhibits a similar relationship with extreme precipitation indices. There is a negative correlation between SCSSMI and extreme precipitation indices, except for R10mm and CWD. Furthermore, the negative correlation is obvious between SCSSMI and Rx1day, Rx5day, SDII, R95p, R99p (significant at 0.01 level), as well as SCSSMI and R25mm (significant at 0.05 level). These results indicate that summer monsoon indices have a significant negative effect on extreme precipitation in WMA during 1960–2019. The weakening of these summer monsoon indices may give rise to a stronger intensity of extreme precipitation.

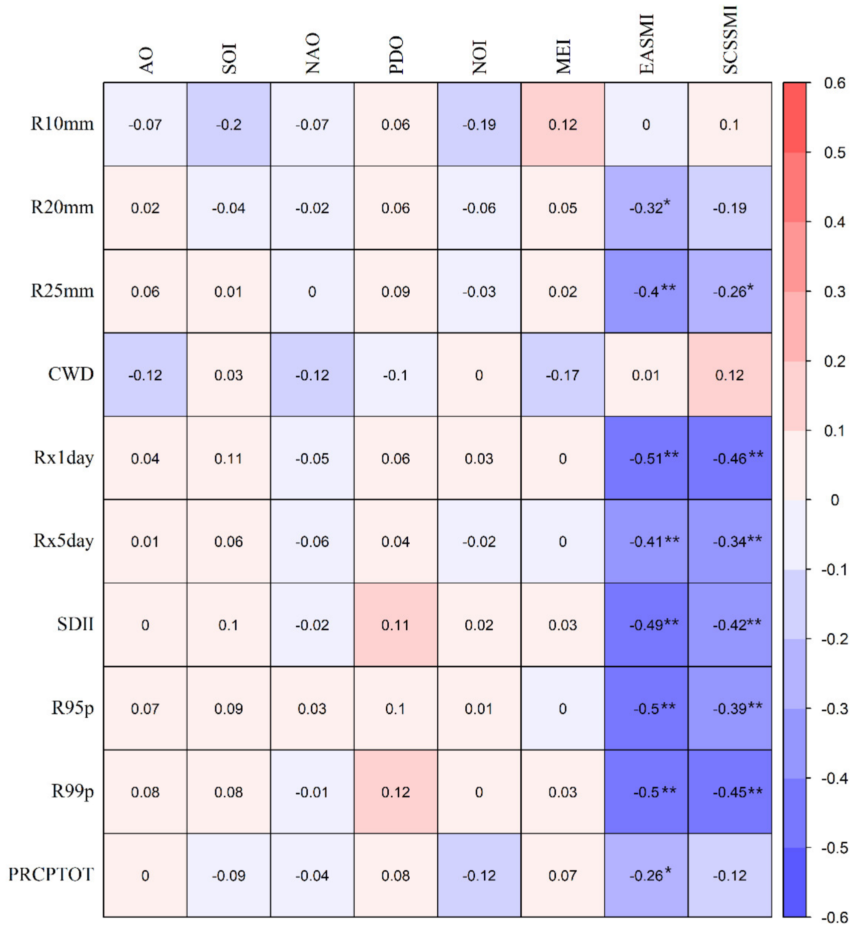


**Figure 10.** Correlation between extreme precipitation and climate variability in WMA. Note: * and ** denote significant correlation at the 0.05 and 0.01 levels, respectively.

In order to further study the spatial pattern of correlations between representative extreme precipitation indices and climate factors with significant influence, the distribution of correlations between extreme precipitation and summer monsoon indices are shown in Figure 11. Moreover, correlations between extreme precipitation and all eight climate variability indices are displayed in Figure S6.

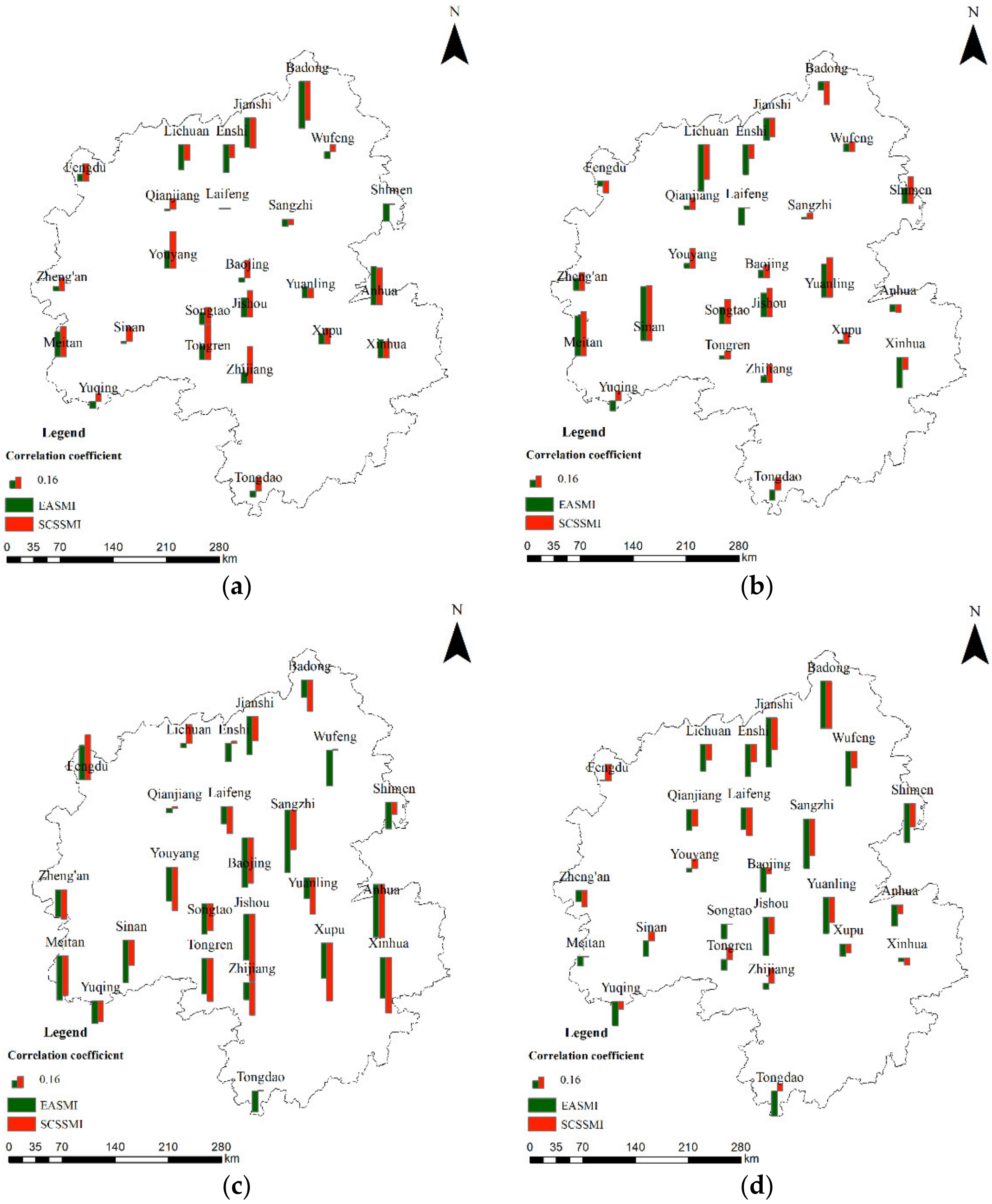


**Figure 11.** Spatial pattern of correlations between summer monsoon indices and extreme precipitation: (**a**) R10mm, (**b**) CWD, (**c**) Rx1day, and (**d**) PRCPTOT in WMA.

Except for the stations located in the north part of WMA, the correlation between summer monsoon indices and R10mm, CWD is positive at most stations. However, there is negative correlation between summer monsoon indices and intensity-based extreme precipitation indices (represented by Rx1day, PRCPTOT). Meanwhile, except for PRCP-

TOT, the correlation between SCSSMI and extreme precipitation at most stations is more significant compared with EASMI.

## 5. Discussion

The frequent occurrence of extreme events is closely related with precipitation distribution, especially the spatial and temporal distribution of the extreme precipitation event [50]. The extreme precipitation events will increase the risk of flood and aggravate the pressure of regional water resources' management [51]. Especially in mountainous areas, extreme precipitation is one of the most dangerous causes of natural disasters, which often induces high-frequency and high-intensity natural disasters, such as floods, landslides, and debris flow. In previous studies, the spatial distribution of extreme precipitation shows remarkable regional differences. An increasing trend is found in the middle and lower reaches of the Yangtze River, South China, and Northwest China, while a decreasing trend occurs in Northeast China, North China, and a part of Southwest China [52,53]. In our study, extreme precipitation in WMA, which belongs to the middle and upper reaches of the Yangtze River, suggests shorter duration and stronger intensity. Rx1day, R95p, R99p, and SDII show a significant increasing trend, while CWD demonstrates an apparent decreasing trend. These findings are in accord with [23,30]. They detected significantly increasing trends of extreme precipitation intensities and decreasing trends of consecutive wet days in the Yangtze River Basin. Furthermore, R20mm and R25mm tend to increase in the middle and east of WMA, where there are areas with relatively low topography and high extreme precipitation intensity. In the context of abrupt analysis for China, extreme precipitation events experienced a sudden change in the early 1990s [52]. However, in the Yangtze River Basin, the abrupt of extreme precipitation intensity and extreme precipitation occurred in the mid-1980s, according to Su et al. [25] and Wang et al. [53]. In our study, significant abrupt changes in extreme precipitation indices in WMA mainly occurred in the 1980s–1990s, which is not very consistent with the relevant research conclusions. This could be partly explained by different datasets and different abrupt test methods. Additionally, regional and local difference may contribute to the inconsistent results. Therefore, it is necessary to further study the internal variation characteristics and reasons for the changes of extreme precipitation.

The potential causes of spatial and temporal heterogeneity in variations of precipitation extremes may include thermodynamic, dynamic factors and local effects. We found all extreme precipitation indices except CWD in WMA to be well correlated with longitude and elevation rather than latitude, which is in accord with Sun [47] and Li et al. [23], albeit without discussion in detail. We consider that the enhanced discrepancy in the thermal properties of land and sea due to climate warming may be part of the reason. Meanwhile, apart from the high elevation in the north and west part, WMA is dominated by small and medium relief mountains. The complex mountainous distribution may lead to different degrees of influence by ocean water vapor in WMA, therefore extreme precipitation is well correlated with longitude rather than latitude. However, in other mountainous area, such as the Qingba mountain area, both longitude and latitude significantly impact the extreme precipitation in Qinba mountains [18].

Global warming tends to enhance the intensities of extreme precipitation in WMA, which is consistent with the results in the Yangtze River Basin [23,31]. Moreover, Li et al. [23] pointed out that global warming has a tendency to increase frequencies of precipitation extremes in the Yangtze River Basin. Although WMA belongs to the upper and middle reaches of the Yangtze River Basin, we found different responses of extreme precipitation frequency to climate warming. Global warming tends to raise the frequency of precipitation in the east of WMA, but reduces the frequency of precipitation in the west of WMA. It indicates that the previous studies on the Yangtze River Basin are not adequate to provide detailed information about precipitation extremes in WMA because of the spatial heterogeneity and inconsistency. The effects of local warming on extreme precipitation are not exactly the same as that of global warming on precipitation extremes. Local warming is likely to decrease the frequency of extreme precipitation, the maximum length of wet days, annual total precipitation, and very wet days precipitation. This might lie in the decreased relative humidity because of local warming, which could affect the precipitation trigger and reduce the extreme precipitation [23].

Previous studies have reported that the East Asian summer monsoon (EASM) experienced a weakening tendency since the end of the 1970s [54,55]. This weakening was manifested as tendencies toward increasing excessive rainfall in South China, along the Yangtze River [56]. In the weakened EASM year, the southwest wind of the western anticyclone directly transports the water vapor from the South China Sea to the Yangtze River basin, leading to an increase in precipitation extremes. In this study, EASMI and SCSSMI have a significant negative influence on extreme precipitation in WMA. The weakening of summer monsoon indices leads to stronger intensity of extreme precipitation. Therefore, the summer monsoon is an important and main reason of extreme precipitation changes in WMA. Meanwhile, the saturation vapor pressure of the atmosphere will increase if the temperature increases [57]. Then, the atmosphere can hold more moisture, which results in more precipitation in an extreme event [58], and the geographic position and topographical features of WMA reinforced the effect. In July, the summer monsoon front is coupled to the mountain alignment, extending from the southwest to the northeast along the Wuling Mountain. The summer monsoon passes through the entire WMA from the south to the north and is blocked by the mountains; then, part of the air mass sinks and mixes with surface heat radiation and transpiration vapor to produce precipitations. Furthermore, the movement of the southwest climatic front coincides with the direction of Wuling Mountain, and the areas where the southern and northern climatic front meets overlap with the distribution of Wuling Mountain. Thus, coupled with topographical features of WMA, summer monsoon indices show control and significant influence on the precipitation extremes in WMA. Additionally, a previous study found that ENSO affects the variability of precipitation extremes of the YRB in both the current year and the coming year [23]. Lv et al. [31] found that ENSO had negative correlation with the winter maximum daily precipitation in the YRB. However, there is no obvious influence of ENSO on extreme precipitation indices detected in this study. The possible reason for this is that a different index was used to quantify the condition of ENSO. There are so many indices used to reflect the impact of ENSO, such as MEI, the Oceanic Niño Index (ONI), sea surface temperature (SST), and so on. The selection of different indexes may produce different results. Moreover, the climate variability index of different time scales put more uncertainty to the correlation between extreme precipitation and climate variability. Under the complicated influence of multiple factors, the drivers and reasons of extreme precipitation changes remain poorly understood [59]. More investigation should focus on the mechanisms responsible for extreme precipitation changes.

## 6. Conclusions

Based on long-term meteorological observation data at 25 stations in Wuling Mountain Area during 1960–2019, this paper presented a comprehensive study of trends and abrupt changes of extreme precipitation. The influence of geographic factors, global warming, local warming, and climate variability are investigated to explore the potential driving factors for the variations of precipitation extremes in WMA. The main conclusions are as follows.

(1) The results show that extreme precipitation intensities (Rx1day, R95p, and R99p) and average precipitation intensity (SDII) increased significantly in WMA during 1960–2019. On the contrary, the maximum duration of wet days (CWD) decreases obviously during the same period. Frequency-based precipitation indices (R10mm, R20mm, R25mm) reduce at most stations, while increasing trends of frequency-based precipitation indices display on the average regional scale. These indicate extreme precipitation with shorter duration and stronger intensity in WMA, which might increase the risk of floods and the resulting landslides and debris flows over WMA,

especially in the middle and east part of WMA, where the elevation is relatively low, but where the intensity and frequency of precipitation extremes tend to increase;

(2) There is no significant abrupt examined for R20mm, R25mm, SDII, or PCRPTOT in WMA during 1960–2019. Significant abrupt changes for other extreme precipitation indices mainly occurred in the 1980s–1990s, and there was an abrupt detected at Qianjiang and Sinan for CWD in the 1970s. The stations with obvious abrupt changes in Rx1day, Rx5day, and R99p are located in the high-value area of extreme precipitation in WMA; yet, sites with a significant abrupt of CWD was mainly distributed in the middle region of WMA;

(3) Extreme precipitation indices except CWD are significantly positively correlated with annual total precipitation, and CWD is weakly associated with other extreme precipitation indicators except R10mm. Geographic factors, longitude, and elevation instead of latitude markedly affect extreme precipitation indices, except for CWD, in WMA. Precipitation extremes tend to decrease from east to west. Meanwhile, the extreme precipitation decreases with an increase in elevation. These results are correspondent with spatial patterns of average annual extreme precipitation indices over WMA. Global warming has a tendency to increase the intensities (Rx1day, Rx5day, R95p, R99p, and SDII) of extreme precipitation and decrease the maximum consecutive wet days (CWD) across WMA. Besides, climate warming tends to raise the frequency of precipitation in the east of WMA, but reduces the frequency of precipitation in the west of WMA. The effects of local warming on extreme precipitation are not exactly the same as that of global warming on precipitation extremes. Local warming is likely to decrease the frequency of extreme precipitation, the maximum length of wet days, annual total precipitation, and very wet days precipitation. However, the opposite effects of local temperature may occur on maximum one-day precipitation, extremely very wet days precipitation, and precipitation intensity. Different climate factors exert different effects on precipitation extremes. The influence of AO, SOI, NAO, PDO, NOI, and MEI on extreme precipitation is relatively weak in WMA. Compared with these climate variability indices, summer monsoon indices, such as EASMI and SCSSMI, have the most obvious impact on the extreme precipitation in WMA during 1960–2019. The weakening of these summer monsoon indices tends to bring the stronger intensity of extreme precipitation. The findings of this study highlight that it is essential to systematically explore the possible driving factors of variations in precipitation extremes in WMA, which is critical and helpful for natural disaster prevention and reduction and adaptive management in this region.

The findings have displayed a clear spatiotemporal variation pattern of precipitation extreme in WMA and have provided deeper understanding of the drivers and reasons of extreme precipitation changes in mountain area. However, there are limitations of this study. Only linear relations are used to measure the connections between extreme precipitation and potential driving factors. However, their relationship may be nonlinear. Future investigation should focus on the nonlinear relationship between precipitation and influencing factors. Meanwhile, the combined effects of two factors or more factors are worth paying attention to. More importantly, the physical mechanism of the potential drivers on extreme precipitation is required in future work.

**Supplementary Materials:** The following supporting information can be downloaded at: https://www.mdpi.com/article/10.3390/su14148312/s1, Figure S1: Spatial variations of annual average extreme precipitation indices (a) R20mm (b) R25mm (c) Rx5day (d)SDII (e)R95p (f)R99p in WMA. Figure S2: Spatial distribution of trends in extreme precipitation indices (a) R20mm (b) R25mm (c) Rx5day (d) SDII (e) R95p (f) R99p in WMA. Figure S3: Spatial distribution of abrupt changes in extreme precipitation indices (a) R10mm, (b) R20mm, (c) R25mm, (d) CWD, (e) Rx1day, (f) Rx5day, (g) SDII, (h) R95p, (i) R99p, (j) PRCPTOT in WMA. Figure S4: Spatial pattern of correlation between global temperature and extreme precipitation indices (a) R20mm (b) R25mm (c) Rx5day (d) SDII (e) R95p (f) R99p in WMA. Figure S5: Spatial pattern of correlation between local temperature and extreme precipitation indices (a) R20mm (b) R25mm (c) Rx5day (d) SDII (e) R95p (f) R99p in WMA. Figure S6: Spatial pattern of correlations between extreme precipitation and climate variability in WMA.

**Author Contributions:** Conceptualization, H.D. and J.X.; Data curation, Y.L. and J.L.; Formal analysis, H.D.; Methodology, H.D. and Y.Y.; Writing—original draft, H.D.; Writing—review and editing, J.X. All authors have read and agreed to the published version of the manuscript.

**Funding:** The study was supported by the Fundamental Research Funds for the Central Universities of South-Central Minzu University (Grant Number: CZD21005) and the National Natural Science Foundation of China (Grant Number: 41901235).

**Institutional Review Board Statement:** Not applicable.

**Informed Consent Statement:** Not applicable.

**Data Availability Statement:** Not applicable.

**Acknowledgments:** We thank the anonymous reviewers for their constructive feedback.

**Conflicts of Interest:** The authors declare no conflict of interest.

## References


1. Madakumbura, G.D.; Thackeray, C.W.; Norris, J.; Goldenson, N.; Hall, A. Anthropogenic influence on extreme precipitation over global land areas seen in multiple observational datasets. *Nat. Commun.* **2021**, *12*, 3944. [CrossRef] [PubMed]
2. Khaing, Z.M.; Zhang, K.; Sawano, H.; Shrestha, B.; Sayama, T.; Nakamura, K. Flood hazard mapping and assessment in data-scarce Nyaungdon area, Myanmar. *PLoS ONE* **2019**, *14*, e0224558. [CrossRef] [PubMed]
3. Liu, S.; Huang, S.; Xie, Y.; Leng, G.; Huang, Q.; Wang, L.; Xue, Q. Spatial-temporal changes of rainfall erosivity in the Loess Plateau, China: Changing patterns, causes and implications. *Catena* **2018**, *166*, 279–289. [CrossRef]
4. Wang, S.; Zhang, K.; van Beek, L.P.; Tian, X.; Bogaard, T.A. Physically-based landslide prediction over a large region: Scaling low-resolution hydrological model results for high resolution slope stability assessment. *Environ. Modell. Softw.* **2020**, *124*, 104607. [CrossRef]
5. Shao, Y.; Mu, X.; He, Y.; Sun, W.; Zhao, G.; Gao, P. Spatiotemporal variations of extreme precipitation events at multi-time scales in the Qinling-Daba mountains region, China. *Quat. Int.* **2019**, *525*, 89–102. [CrossRef]
6. Morrison, A.; Villarini, G.; Zhang, W.; Scoccimarro, E. Projected changes in extreme precipitation at sub-daily and daily time scales. *Glob. Planet. Chang.* **2019**, *182*, 103004. [CrossRef]
7. Cardell, M.F.; Amengual, A.; Romero, R.; Ramis, C. Future extremes of temperature and precipitation in Europe derived from a combination of dynamical and statistical approaches. *Int. J. Climatol.* **2020**, *40*, 4800–4827. [CrossRef]
8. Donat, M.G.; Lowry, A.L.; Alexander, L.V.; O'Gorman, P.A.; Maher, N. More extreme precipitation in the world's dry and wet regions. *Nat. Clim. Chang.* **2016**, *6*, 508–513. [CrossRef]
9. Zhou, B.; Xu, Y.; Wu, J.; Dong, S.; Shi, Y. Changes in temperature and precipitation extreme indices over China: Analysis of a high-resolution grid dataset. *Int. J. Climatol.* **2016**, *36*, 1051–1066. [CrossRef]
10. Alexander, L.V.; Zhang, X.; Peterson, T.C.; Caesar, J.; Gleason, B.; Tank, A.M.G.K.; Haylock, M.; Collins, D.; Trewin, B.; Rahimzadeh, F.; et al. Global observed changes in daily climate extremes of temperature and precipitation. *J. Geophys. Res. Atmos.* **2006**, *111*, 1042–1063. [CrossRef]
11. Fang, J.; Yang, W.; Luan, Y.; Du, J.; Lin, A.; Zhao, L. Evaluation of the TRMM 3B42 and GPM IMERG products for extreme precipitation analysis over China. *Atmos. Res.* **2019**, *223*, 24–38. [CrossRef]
12. Guan, Y.; Zheng, F.; Zhang, X.; Wang, B. Trends and variability of daily precipitation and extremes during 1960–2012 in the Yangtze River Basin, China. *Int. J. Climatol.* **2017**, *37*, 1282–1298. [CrossRef]
13. Gao, T.; Wang, H. Trends in precipitation extremes over the Yellow River basin in North China: Changing properties and causes. *Hydrol. Processes* **2017**, *31*, 2412–2428. [CrossRef]
14. Mei, C.; Liu, J.; Chen, M.T.; Wang, H.; Li, M.; Yu, Y. Multi-decadal spatial and temporal changes of extreme precipitation patterns in northern China (Jing-Jin-Ji district, 1960–2013). *Quat. Int.* **2018**, *476*, 1–13. [CrossRef]
15. Wentz, F.J.; Ricciardulli, L.; Hilburn, K.; Mears, C. How much more rain will global warming bring? *Science* **2007**, *317*, 233–235. [CrossRef]
16. Allan, R.P.; Soden, B.J. Atmospheric warming and the amplification of precipitation extremes. *Science* **2008**, *321*, 1481–1484. [CrossRef]
17. Alexander, L.V.; Uotila, P.; Nicholls, N. Influence of sea surface temperature variability on global temperature and precipitation extremes. *J. Geophys. Res. Atmos.* **2009**, *114*, D18116. [CrossRef]
18. Wang, L.; Chen, S.; Zhu, W.; Ren, H.; Zhang, L.; Zhu, L. Spatiotemporal variations of extreme precipitation and its potential driving factors in China's North-South Transition Zone during 1960–2017. *Atmos. Res.* **2021**, *252*, 105429. [CrossRef]

19. IPCC. 2021: Summary for Policymakers. In *Climate Change 2021: The Physical Science Basis. Contribution of Working Group I to the Sixth Assessment Report of the Intergovernmental Panel on Climate Change*; Masson-Delmotte, V.P., Zhai, A., Pirani, S.L., Connors, C., Péan, S., Berger, N., Caud, Y., Chen, L., Goldfarb, M.I., Gomis, M., et al., Eds.; Cambridge University Press: Cambridge, UK, 2021; *in press*.
20. Otto, F.E.L.; van Oldenborgh, G.J.; Eden, J.; Stott, P.A.; Karoly, D.J.; Allen, M.R. The attribution question. *Nat. Clim. Chang.* **2016**, *6*, 813–816.
21. Perlwitz, J.; Knutson, T.; Kossin, J. Large-scale circulation and climate variability. In *Climate Science Special Report: Fourth National Climate Assessment*; Wuebbles, D.J., Fahey, D.W., Hibbard, K.A., Dokken, D.J., Stewart, B.C., Maycock, T.K., Eds.; U.S. Global Change Research Program: Washington, DC, USA, 2017; Volume I, pp. 161–184. [CrossRef]
22. Mondal, A.; Mujumdar, P.P. Modeling non-stationarity in intensity, duration and frequency of extreme rainfall over India. *J. Hydrol.* **2015**, *521*, 217–231. [CrossRef]
23. Li, X.; Zhang, K.; Gu, P.R.; Feng, H.T.; Yin, Y.F.; Chen, W.; Cheng, B.C. Changes in precipitation extremes in the Yangtze River Basin during 1960–2019 and the association with global warming, ENSO, and local effects. *Sci. Total Environ.* **2021**, *760*, 144244. [CrossRef]
24. Papalexiou, S.M.; Montanari, A. Global and regional increase of precipitation extremes under global warming. *Water Resour. Res.* **2019**, *55*, 4901–4914. [CrossRef]
25. Su, B.D.; Gemmer, M.; Jiang, T. Spatial and temporal variation of extreme precipitation over the Yangtze River Basin. *Quat. Int.* **2008**, *186*, 22–31. [CrossRef]
26. Nie, C.; Li, H.; Yang, L.; Ye, B.; Dai, E.; Wu, S.; Liu, Y.; Liao, Y. Spatial and temporal changes in extreme temperature and extreme precipitation in Guangxi. *Quat. Int.* **2012**, *263*, 162–171. [CrossRef]
27. Zhang, K.X.; Pan, S.; Cao, L.; Wang, Y.; Zhao, Y.; Zhang, W. Spatial distribution and temporal trends in precipitation extremes over the Hengduan Mountains region, China, from 1961 to 2012. *Quat. Int.* **2014**, *349*, 346–356. [CrossRef]
28. Zhang, X.; Chen, Y.; Fang, G.; Li, Y.; Li, Z.; Wang, F.; Xia, Z. Observed changes in extreme precipitation over the Tienshan Mountains and associated large-scale climate teleconnections. *J. Hydrol.* **2022**, *606*, 127457. [CrossRef]
29. Shang, Z.K.; Shao, K. Natural disasters in Wuling Mountainous Area. *Minzu Trib.* **2020**, *2*, 59–66. (In Chinese)
30. Li, P.; Yu, Z.; Jiang, P.; Wu, C. Spatiotemporal characteristics of regional extreme precipitation in Yangtze River Basin. *J. Hydrol.* **2021**, *603*, 126910. [CrossRef]
31. Lv, M.; Wu, S.J.; Chen, J.; Chen, C.; Wen, Z.; Huang, Y. Changes in extreme precipitation in the Yangtze River basin and its association with global mean temperature and ENSO. *Int. J. Climatol.* **2018**, *38*, 1989–2005.
32. Miao, C.; Duan, Q.; Sun, Q.; Lei, X.; Li, H. Non-uniform changes in different categories of precipitation intensity across China and the associated large-scale circulations. *Environ. Res. Lett.* **2019**, *14*, 025004. [CrossRef]
33. Gao, T.; Zhang, Q.; Luo, M. Intensifying effects of El Niño events on winter precipitation extremes in southeastern China. *Clim. Dyn.* **2020**, *54*, 631–648. [CrossRef]
34. Yu, H.; Wang, L.; Yang, R.; Yang, M.; Gao, R. Temporal and spatial variation of precipitation in the Hengduan Mountains region in China and its relationship with elevation and latitude. *Atmos. Res.* **2018**, *213*, 1–16. [CrossRef]
35. Croitoru, A.E.; Piticar, A.; Burada, D.C. Changes in precipitation extremes in Romania. *Quat. Int.* **2016**, *415*, 325–335. [CrossRef]
36. You, Q.L.; Kang, S.C.; Aguilar, E.; Pepin, N.; Fluegel, W.A.; Yan, Y.P.; Xu, Y.W.; Zhang, Y.J.; Huang, J. Changes in daily climate extremes in China and their connection to the large scale climate variability during 1961–2003. *Clim. Dyn.* **2011**, *36*, 2399–2417. [CrossRef]
37. Hu, W.; Yao, J.; He, Q.; Chen, J. Changes in precipitation amounts and extremes across Xinjiang (northwest China) and their connection to climate indices. *PeerJ* **2021**, *9*, e10792. [CrossRef]
38. Du, H.; Xia, J.; Zeng, S.D. Regional frequency analysis of extreme precipitation and its spatio-temporal characteristics in the Huai River Basin, China. *Nat. Hazards* **2014**, *70*, 195–215. [CrossRef]
39. Song, X.M.; Zhang, J.Y.; Zou, X.; Zhang, C.; AghaKouchak, A.; Kong, F. Changes in precipitation extremes in the Beijing metropolitan area during 1960–2012. *Atmos. Res.* **2019**, *222*, 134–153. [CrossRef]
40. Yue, S.; Pilon, P.; Phinney, B.; Cavadias, G. The influence of autocorrelation on the ability to detect trend in hydrological series. *Hydrol. Process.* **2002**, *16*, 1807–1829. [CrossRef]
41. Liu, S.Y.; Huang, S.; Huang, Q.; Xie, Y.; Leng, G.; Luan, J.; Song, X.; Wei, X.; Li, X. Identification of the non-stationarity of extreme precipitation events and correlations with large-scale ocean-climate variability patterns: A case study in the Wei River Basin, China. *J. Hydrol.* **2017**, *548*, 184–195. [CrossRef]
42. Mann, H.B. Nonparametric tests against trend. *Econometrica* **1945**, *13*, 245–259. [CrossRef]
43. Kendall, M.G. *Rank Correlation Methods*; Griffin: London, UK, 1975.
44. Gu, X.H.; Zhang, Q.; Li, J.F.; Singh, V.P.; Sun, P. Impact of urbanization on nonstationarity of annual and seasonal precipitation extremes in China. *J. Hydrol.* **2019**, *575*, 638–655. [CrossRef]
45. Zhang, Y.; Li, C.B.; Wang, L.M. Application and comparison of several test methods for changepoints diagnosis in streamflow variations. *Water Resour. Hydro. Eng.* **2020**, *51*, 38–47.
46. Pettitt, A.N. A non-parametric approach to the change-point problem. *Appl. Stat.* **1979**, *28*, 126–135. [CrossRef]
47. Sun, L. Drought Monitoring and Early Warning in Mountain and Hilly Area—A Case of Wuling Mountain Area. Ph.D. Dissertation, China Agricultural University, Beijing, China, 2014.

48. Wotling, G.; Bouvier, C.; Danloux, J.; Fritsch, J.M. Regionalization of extreme precipitation distribution using the principal components of the topographical environment. *J. Hydrol.* **2000**, *233*, 86–101. [CrossRef]
49. Zhang, Q.; Li, J.F.; Chen, X.H.; Bai, Y.G. Spatial variability of probability distribution of extreme precipitation in Xinjiang. *Acta Geogr. Sin.* **2011**, *66*, 3–12.
50. Ahmed, K.; Shahid, S.; Chung, E.S.; Wang, X.J.; Bin Harun, S. Climate change uncertainties in seasonal drought severity-area-frequency curves: Case of arid region of Pakistan. *J. Hydrol.* **2019**, *570*, 473–485. [CrossRef]
51. Gao, T.; Xie, L. Study on Progress of the Trends and Physical causes of Extreme Precipitation in China during the Last 50 Years. *Adv. Earth Sci.* **2014**, *29*, 577–589.
52. Long, Y.Y.; Fan, G.Z.; Duan, L.; Feng, W.; Wang, Q.; Li, F.; Zhang, Y. A Study on the Characteristics of Summertime Extreme Precipitation Events over China in Recent 54 Years. *Clim. Environ. Res.* **2016**, *21*, 429–438. (In Chinese)
53. Wang, J.; Jiang, Z.H.; Yan, M.L.; Zhang, J.L. Trends of extreme precipitation indices in the mid-lower Yangtze River valley of China during 1960-2005. *Sci. Meteorol. Sin.* **2008**, *28*, 384–388. (In Chinese)
54. Liu, H.W.; Zhou, T.J.; Zhu, Y.X.; Lin, Y. The strengthening East Asia summer monsoon since the early 1990s. *Chin. Sci. Bull.* **2012**, *57*, 1553–1558. [CrossRef]
55. Chen, D.; Zhou, F.; Dong, Z.; Zeng, A.Y.; Ou, T.; Fang, K. A tree-ring $\delta^{18}O$ based reconstruction of East Asia summer monsoon over the past two centuries. *PLoS ONE* **2020**, *15*, e0234421. [CrossRef]
56. Ding, Y.; Wang, Z.; Sun, Y. Inter-decadal variation of the summer precipitation in east China and its association with decreasing Asian summer monsoon. Part I: Observed evidences. *Int. J. Climatol.* **2007**, *28*, 1139–1161. [CrossRef]
57. Trenberth, K.E. Changes in precipitation with climate change. *Clim. Res.* **2011**, *47*, 123–138. [CrossRef]
58. Sharma, A.; Wasko, C.; Lettenmaier, D.P. If precipitation extremes are increasing, why aren't floods? *Water Resour. Res.* **2018**, *54*, 8545–8551. [CrossRef]
59. Tandon, N.F.; Zhang, X.; Sobel, A.H. Understanding the dynamics of future changes in extreme precipitation intensity. *Geophys. Res. Lett.* **2018**, *45*, 2870–2878. [CrossRef]